

# Qubit metrology and decoherence

Anil Shaji and Carlton M. Caves

*Department of Physics and Astronomy, University of New Mexico, Albuquerque, NM 87131*

(Dated: February 1, 2008)

Quantum properties of the probes used to estimate a classical parameter can be used to attain accuracies that beat the standard quantum limit. When qubits are used to construct a quantum probe, it is known that initializing  $n$  qubits in an entangled “cat state,” rather than in a separable state, can improve the measurement uncertainty by a factor of  $1/\sqrt{n}$ . We investigate how the measurement uncertainty is affected when the individual qubits in a probe are subjected to decoherence. In the face of such decoherence, we regard the rate  $R$  at which qubits can be generated and the total duration  $\tau$  of a measurement as fixed resources, and we determine the optimal use of entanglement among the qubits and the resulting optimal measurement uncertainty as functions of  $R$  and  $\tau$ .

PACS numbers: 03.65.Ta, 06.20.-f, 03.65.Yz, 03.67.-a

Keywords: quantum metrology, decoherence, Braunstein-Caves inequality

## I. INTRODUCTION

This paper considers the question of quantum limits on estimating the value of a parameter that influences the state of a physical system [1, 2, 3, 4, 5, 6, 7, 8, 9]. We call this system, which is intrinsically quantum mechanical, a *probe*, because it is used to probe the value of the parameter. The accuracy with which the parameter can be estimated is determined by the initial quantum state of the probe, the type of interaction by which the parameter influences the state of the probe, and the readout measurement that is used to extract information from the probe.

In this paper the probe is always a collection of  $n$  qubits. We assume that there is sufficient control over the probe qubits to initialize the probe in any separable or entangled pure state. We let  $g$  denote the parameter we are estimating. The effect of  $g$  on the  $j$ th probe qubit is described by the Hamiltonian

$$H_j(g) = \frac{1}{2}g\sigma_{z;j} . \quad (1.1)$$

Here  $\sigma_{z;j}$  denotes the Pauli  $z$  operator for the  $j$ th qubit; similarly,  $\sigma_{x;j}$  and  $\sigma_{y;j}$  denote the other two Pauli operators. The parameter  $g$ , which has units of frequency (we choose  $\hbar = 1$ ), is a coupling strength. The Hamiltonian (1.1) generates a rotation about the  $z$  axis of the qubit’s Bloch sphere. The overall influence of the parameter on the probe is given by the Hamiltonian

$$H = \sum_{j=1}^n H_j(g) = \frac{1}{2}g \sum_{j=1}^n \sigma_{z;j} . \quad (1.2)$$

The value of  $g$  is to be deduced from the change in the state of the probe. For simplicity, we assume that the probe qubits do not have any free Hamiltonian evolution.

Giovannetti, Lloyd, and Maccone [9] have analyzed a general scheme of this type. Their theoretical framework involves estimating a dimensionless parameter  $\varphi$ , introduced on the probe through a unitary transformation  $U = e^{-ih\varphi}$ , with  $h = \sum_{j=1}^n h_j$ . They do not identify  $h$  as a Hamiltonian; rather it is treated as an arbitrary operator that is the generator of translations in the variable  $\varphi$ . The connection between our scheme and theirs is established by identifying  $h = H/g$  ( $h_j = H_j/g$ ) and  $\varphi = gT$ , where  $T$  is the time for which the Hamiltonian (1.2) acts on the probe.

The chief objective of our analysis, following [10], is to expand the discussion in [9] by investigating how decoherence impacts the accuracy with which the parameter can be determined. Thus we assume that in addition to the Hamiltonians  $H_j(g)$ , the probe qubits are subject to other influences that can lead to decoherence. For the decoherence models we consider, the effects of decoherence manifest themselves at a readily identifiable rate, which we denote as  $\gamma$ . To make the analysis meaningful, we must impose additional constraints on the probes, since we can always make decoherence irrelevant by estimating  $g$  using a procedure that is completed in a time much shorter than the time  $\gamma^{-1}$  over which decoherence has a significant effect. Thus we assume that qubits are made available and initialized into probes at a rate  $R$ . What we have in mind is that each probe is assembled in a time  $n/R$  and is then sent immediately through a quantum channel, where it is subjected to the Hamiltonian (1.2) for a time  $T$ . If we use  $\nu$  probes to estimate  $g$ , so that the total number of qubits is

$$N = \nu n, \quad (1.3)$$

the total time required is

$$\tau = \nu n/R + T, \quad (1.4)$$

provided that the quantum channel can accommodate more than one probe at a time. In our analysis, we assume that the parameter must be determined in the fixed time  $\tau$  ( $\tau^{-1}$  can be thought of roughly as the bandwidth over which a time-varying  $g$  is estimated), that the qubit supply rate  $R$  is a fixed resource, and that the decoherence rate  $\gamma$  is a constant. We vary the interaction time  $T$  and the number of qubits in each probe,  $n = R(\tau - T)/\nu$ , to achieve the best accuracy in determining  $g$ .

A measurement scheme of the sort discussed here appears in slightly modified forms in several problems of practical importance, such as clock synchronization [11, 12, 13, 14, 15, 16], reference-frame alignment [17, 18], phase estimation [19, 20, 21], frequency measurements [10, 22, 23], and position measurements [24, 25].

The accuracy with which  $g$  can be estimated is closely connected to the distinguishability of neighboring states of the quantum probe. This connection is quantified by the generalized uncertainty relations formulated by Braunstein, Caves, and Milburn [6]. As in [9], we use these generalized uncertainty relations to describe the optimal accuracy of parameter estimation.

In Sec. II, we review the formalism of generalized uncertainty relations in the forms suitable for our analysis and discuss briefly aspects of the assumptions we make about resources and time

scales in our measurement protocol. Section III reviews the accuracy that can be achieved in the absence of decoherence, and Sec. IV investigates how the achievable accuracies are affected by a general qubit decoherence process. The final section provides a short discussion of our results.

## II. GENERALIZED UNCERTAINTY RELATIONS

As a consequence of spending a time  $T$  in the quantum channel, the quantum state of the probe changes from an initial state  $\rho_0$  to a final state

$$\rho(g, T) = e^{-iHT} \mathcal{A}_T(\rho_0) e^{iHT} = e^{-ihgT} \mathcal{A}_T(\rho_0) e^{ihgT}, \quad (2.1)$$

where  $\mathcal{A}_T$  is the superoperator that describes the cumulative effect of decoherence in the channel. The final state can always be written in the form (2.1), by going to an interaction picture relative to the Hamiltonian (1.2), but in doing so, the decoherence superoperator,  $\mathcal{A}_T$ , generally becomes dependent on  $g$ . In our analysis, however, we assume all decoherence processes to be invariant under rotations about the  $z$  axis (we also assume that the decoherence is independent and identical from one qubit to the next), which implies that  $\mathcal{A}_T$  is independent of  $g$  and also means that  $\mathcal{A}_T$  commutes with  $e^{-ihgT}$ , i.e.,  $\rho(g, T) = \mathcal{A}_T(e^{-ihgT} \rho_0 e^{ihgT})$ . The final state contains the information about the value of  $g$ . The accuracy with which we can distinguish the state  $\rho(g, T)$  from neighboring states on the one-parameter path parametrized by  $g$  controls the accuracy in the estimate of  $g$ .

From the results of measurements on a set of  $\nu$  probes, we obtain an estimate  $g_{\text{est}}$  for the value of  $g$ . We can quantify the statistical deviation of the estimate from the true value of  $g$  by the units-corrected deviation from the actual value,

$$\delta g \equiv \left\langle \left( \frac{g_{\text{est}}}{|d\langle g_{\text{est}} \rangle_g / dg|} - g \right)^2 \right\rangle^{1/2}, \quad (2.2)$$

introduced in [3, 6]. A lower bound on  $\delta g$  is given by the generalized uncertainty relation [1, 2, 3, 4, 5, 6],

$$\delta g \geq \frac{1}{\sqrt{\nu} (ds/dg)}, \quad (2.3)$$

where  $ds$  is the “statistical distance” between neighboring quantum states along the trajectory parametrized by  $g$ . The statistical distance is given in terms of the change,

$$d\rho = \frac{d\rho(g, T)}{dg} dg \equiv \rho' dg, \quad (2.4)$$

in  $\rho = \rho(g, T)$  due to a small change  $dg$  in the value of  $g$ :

$$\left( \frac{ds}{dg} \right)^2 = \text{tr}(\rho' \mathcal{L}_\rho(\rho')). \quad (2.5)$$

In the basis  $\{|\alpha\rangle\}$  that diagonalizes  $\rho(g, T) = \sum_\alpha p_\alpha |\alpha\rangle\langle\alpha|$ , the superoperator  $\mathcal{L}_\rho$  takes the form

$$\mathcal{L}_\rho(O) = \sum_{\{\alpha, \beta | p_\alpha + p_\beta \neq 0\}} \frac{2}{p_\alpha + p_\beta} O_{\alpha\beta} |\alpha\rangle\langle\beta|. \quad (2.6)$$

The operator  $\mathcal{L}_\rho(\rho')$  is called the *symmetric logarithmic derivative* [2] because

$$\rho' = \frac{1}{2} \left( \rho \mathcal{L}_\rho(\rho') + \mathcal{L}_\rho(\rho') \rho \right). \quad (2.7)$$

The quantity  $(ds/dg)^2 = \text{tr}[\rho' \mathcal{L}_\rho(\rho')]$  is often called the *quantum Fisher information* [2].

The generalized uncertainty relations are derived using a quantum version of the Cramer-Rao bound [3, 6, 26]. Generally, this bound can be achieved only in the case of an optimal measurement on each probe and, even then, only asymptotically for a large number  $\nu$  of probes, as emphasized by Braunstein [27]. In our analysis, we explicitly exhibit an optimal measurement, and we let  $\nu_{\min}$  denote the number of probes required to approach the bound within some fixed fractional error.

Consider now the continuous path in the space of states of the probe parametrized by  $g$ . Nearby points on this path are related by the derivative

$$\rho' = -iT[h, \rho] = -iT[\hat{h}, \rho] = iT \sum_{\alpha, \beta} (p_\alpha - p_\beta) \hat{h}_{\alpha\beta} |\alpha\rangle\langle\beta|, \quad (2.8)$$

where here and throughout a hat denotes the difference between a quantity and its mean value, i.e.,  $\hat{h} = h - \langle h \rangle$ . Plugged into Eq. (2.6), this gives

$$\mathcal{L}_\rho(\rho') = 2iT \sum_{\alpha, \beta} \frac{p_\alpha - p_\beta}{p_\alpha + p_\beta} \hat{h}_{\alpha\beta} |\alpha\rangle\langle\beta| \quad (2.9)$$

and

$$\left( \frac{ds}{dg} \right)^2 = 4T^2 \Delta^2 \leq 4T^2 (\Delta h)^2, \quad (2.10)$$

where

$$\Delta^2 \equiv \frac{1}{2} \sum_{\alpha, \beta} \frac{(p_\alpha - p_\beta)^2}{p_\alpha + p_\beta} |\hat{h}_{\alpha\beta}|^2 \quad (2.11)$$

and

$$(\Delta h)^2 \equiv \langle \hat{h}^2 \rangle = \frac{1}{2} \sum_{\alpha, \beta} (p_\alpha + p_\beta) |\hat{h}_{\alpha\beta}|^2 \quad (2.12)$$

is the variance of  $h$  with respect to  $\rho(g, T)$ . Notice that in Eqs. (2.9) and (2.11), we can remove the hat from  $h$  without changing anything, whereas in the variance (2.12), we cannot do so. From Eqs. (2.3) and (2.10), we obtain

$$\delta g \geq \frac{1}{\sqrt{\nu} 2T \Delta} \geq \frac{1}{\sqrt{\nu} 2T \Delta h}. \quad (2.13)$$

These are the generalized uncertainty relations in the forms we will use. Notice that when  $\rho(g, T)$  is a pure state, we have  $\Delta = \Delta h$ , and thus equality holds in Eq. (2.10) and in the second inequality in Eq. (2.13). Notice also that in the absence of decoherence (i.e., when  $\mathcal{A}_T$  is the unit superoperator), a pure initial state stays pure, and  $\Delta h$  is independent of  $T$ .

The second (weaker) inequality in Eq. (2.13) is generally easier to work with than the first (stronger) inequality, because computing the uncertainty  $\Delta h$  is usually easier than computing the corresponding term in the first inequality. In the case of an initial pure state in the absence of decoherence, the two inequalities are equivalent. In this case, to minimize the uncertainty in  $g$ , we should initialize the probe in a state in which  $\Delta h$  is maximal. We show in Sec. IV that when there is decoherence in the probe qubits, which changes an initial pure state to a mixed state, the weaker inequality is not very useful, and we are forced to work with the stronger inequality.

For nonGaussian statistics, the quantum Cramer-Rao bound is saturated only in the limit  $\nu \rightarrow \infty$ , i.e., when the measurement process involving an  $n$ -qubit probe is repeated many times. We let  $\nu_{\min}$  denote the minimum number of iterations that are required for the measurement accuracy to approach the quantum Cramer-Rao bound within some fixed fractional error. For the qubit protocols we analyze,  $\nu_{\min}$  is essentially independent of protocol, as we discuss further below when we consider measurements that achieve the bound (2.13); a typical value might be, say, 50. The need to do at least  $\nu_{\min}$  iterations places a constraint,  $\nu \geq \nu_{\min}$ . Together with the constraint that each probe must contain at least one qubit, this gives us the following constraints on  $n$ :

$$1 \leq n = N/\nu \leq N/\nu_{\min} . \quad (2.14)$$

For these constraints to be consistent, it must be true that

$$R(\tau - T) = N \geq \nu_{\min} . \quad (2.15)$$

As we discussed in the Introduction, we assume in our analysis that the parameter must be determined in a fixed time  $\tau = \nu n/R + T$  and that the qubit supply rate  $R$  is a fixed resource. For a particular kind of decoherence, we vary the interaction time  $T$  and the number of qubits in each probe,  $n = R(\tau - T)/\nu$ , to achieve the best accuracy in determining  $g$ .

A different sort of resource that is dependent on the way the probe is initialized is the magnitude of  $\Delta$ . If we assume that the energy spread for each of the qubits is fixed, then a way of getting a large value for  $\Delta$  is to initialize the  $n$  qubits in each probe in an appropriate entangled state. In a sense,  $\Delta$  is itself a measure of the entanglement or quantum coherence available for improving the ability to determine  $g$ .

### III. MEASUREMENT ACCURACY IN THE ABSENCE OF DECOHERENCE

In this section we review the limits on the accuracy of estimating  $g$  in the case where there is no decoherence. From the generalized uncertainty relation, we see that the initial state of the probe has a direct bearing on the optimal accuracy. We look at two very different initial pure states of the probe. In the first case the  $n$  probe qubits are initialized in a product state, and in the second case they are in a collective entangled state. For both cases we compute the limit on the precision with which  $g$  can be estimated. Since there is no decoherence, the probe state remains pure, and the two inequalities in Eq. (2.13) are equivalent, because  $\Delta = \Delta h$ . Thus in this section

we only need to consider  $\Delta h$ . This section also serves to establish our notation and to summarize the results in [9].

### A. Initial pure product state

If the probe is initialized in a pure product state,  $\rho_p$ , of the  $n$  qubits, we have

$$\frac{ds_p}{dg} = \sqrt{\sum_{j=1}^n \left(\frac{ds_j}{dg}\right)^2}, \quad (3.1)$$

as shown in Appendix A (see also [6]). Here and in the following, the subscript  $p$  stands for “product state.” The line element  $ds_p$  is in the space of  $n$ -qubit density operators, while  $ds_j$  are line elements in the space of states of each the  $n$  probe qubits. From Eq. (2.13) we see that the best choice of initial probe state is one that maximizes

$$\Delta = \Delta h = \sqrt{\sum_{j=1}^n (\Delta h_j)^2}, \quad (3.2)$$

where  $(\Delta h_j)^2$  is the variance of  $h_j$  for the  $j$ th qubit. Thus we have to maximize  $\Delta h_j$  for each of the  $n$  qubits, and we do so by initializing each of the  $n$  qubits in a pure state lying in the equatorial plane of the Bloch sphere of states for each qubit. Here we choose initial state

$$|\psi_j\rangle = \frac{1}{\sqrt{2}}(|0_j\rangle + |1_j\rangle) \quad \text{or} \quad \rho_j = \frac{1}{2}(\mathbb{1}_j + \sigma_{x;j}). \quad (3.3)$$

The vectors  $|0_j\rangle$  and  $|1_j\rangle$  denote the eigenstates of  $\sigma_{z;j}$  for the  $j$ th qubit. The initial state of the probe is

$$\rho_p = \bigotimes_{j=1}^n \rho_j = \frac{1}{2^n} \bigotimes_{j=1}^n (\mathbb{1}_j + \sigma_{x;j}). \quad (3.4)$$

The effect of the coupling to the parameter is to rotate the Bloch vector of each of the qubits around the  $\sigma_z$  axis. At time  $T$ , after passage through the channel, the state of each qubit has rotated through an angle  $gT$ , giving a probe state

$$\rho_p(g, T) = \bigotimes_{j=1}^n \rho_j(g, T) = \frac{1}{2^n} \bigotimes_{j=1}^n (\mathbb{1}_j + \sigma_{x;j} \cos gT + \sigma_{y;j} \sin gT). \quad (3.5)$$

We use the evolved state (3.5) in our discussion of achieving the optimal measurement accuracy in Sec. III C. For the present, however, since the variance of  $h_j$  is unchanged by the evolution, we can evaluate it using the initial state (3.3). This gives a variance  $(\Delta h_j)^2 = 1/4$  for each qubit, and thus

$$(\Delta h)^2 = n(\Delta h_j)^2 = \frac{n}{4}. \quad (3.6)$$

The generalized-uncertainty bound on the estimate of  $g$  becomes

$$\delta g \geq \delta g_p = \frac{1}{T\sqrt{\nu n}} = \frac{1}{T\sqrt{N}} = \frac{1}{T\sqrt{R(\tau - T)}} , \quad (3.7)$$

where  $N$  is the total number of qubits used in the measurement scheme, and  $\delta g_p$  is the bound for pure product inputs.

Since the bound depends only on  $N$ , and not separately on  $n$  and  $\nu$ , we can always choose  $n = 1$  without affecting the optimal measurement accuracy. This, of course, is the statement that for product-state inputs, the measurement accuracy is indifferent to whether we regard the qubits as gathered together into multi-qubit probes. To find the optimal bound, all that is left is to adjust the interaction time  $T$  to minimize  $\delta g_p$ . Doing so gives

$$T = \frac{2}{3}\tau \quad (3.8)$$

and thus

$$N = \nu = \frac{1}{3}R\tau . \quad (3.9)$$

That there be enough probes to satisfy  $\nu \geq \nu_{\min}$  requires that  $\frac{1}{3}R\tau \geq \nu_{\min}$ . When  $\frac{1}{3}R\tau < \nu_{\min}$ , the measurement bound is optimized by the choices  $n = 1$  and  $\nu = \nu_{\min}$ . This gives an interaction time  $T = \tau - \nu_{\min}/R$  that decreases with  $\tau$  until  $R\tau = \nu_{\min}$ , at which point it is impossible to obtain and use  $\nu_{\min}$  probes within the overall duration  $\tau$ . This interaction time occurs in every situation we consider, when the measurement protocol is starved of qubits, so we abbreviate it as

$$T_s \equiv \tau - \nu_{\min}/R . \quad (3.10)$$

The optimal bound on measurement accuracy thus takes the form

$$\delta g_p = \begin{cases} \frac{1}{T_s\sqrt{\nu_{\min}}} , & 1 \leq R\tau < 3\nu_{\min} , \\ \frac{3\sqrt{3}/2}{\tau\sqrt{R\tau}} , & 3\nu_{\min} \leq R\tau . \end{cases} \quad (3.11)$$

In our resource-based analysis, in which the overall measurement time  $\tau$  and the rate  $R$  at which qubits can be supplied are the resources, the  $1/\sqrt{R\tau^3}$  scaling is the signature of the *standard quantum limit*. The behavior of the bound for  $1 \leq R\tau < 3\nu_{\min}$  is included for completeness in our subsequent analysis, but is not so important since it expresses what happens when the measurement protocol is starved of qubits.

## B. Initial pure entangled state

If the probe can be initialized in an entangled state, we can obtain bigger values of  $\Delta h$ . The maximum value is obtained by superposing two  $n$ -qubit eigenstates of  $h$  corresponding to the lowest and highest eigenvalues. Thus we initialize the probe in the “cat” state [9]

$$|\Psi_c\rangle = \frac{1}{\sqrt{2}} (|00\dots 0\rangle + |11\dots 1\rangle) , \quad (3.12)$$

denoted by the subscript  $c$ . The initial density operator  $\rho_c = |\Psi_c\rangle\langle\Psi_c|$  can be written in the form

$$\rho_c = \frac{1}{2^{n+1}} \left( \bigotimes_{j=1}^n (\mathbb{1}_j + \sigma_{z;j}) + \bigotimes_{j=1}^n (\mathbb{1}_j - \sigma_{z;j}) + \bigotimes_{j=1}^n (\sigma_{x;j} + i\sigma_{y;j}) + \bigotimes_{j=1}^n (\sigma_{x;j} - i\sigma_{y;j}) \right). \quad (3.13)$$

After passage through the quantum channel, the state of the probe becomes

$$\begin{aligned} \rho_c(g, T) = \frac{1}{2^{n+1}} & \left( \bigotimes_{j=1}^n (\mathbb{1}_j + \sigma_{z;j}) + \bigotimes_{j=1}^n (\mathbb{1}_j - \sigma_{z;j}) \right. \\ & \left. + e^{-ingT} \bigotimes_{j=1}^n (\sigma_{x;j} + i\sigma_{y;j}) + e^{ingT} \bigotimes_{j=1}^n (\sigma_{x;j} - i\sigma_{y;j}) \right). \end{aligned} \quad (3.14)$$

We use this form in our discussion of achievability in Sec. III C. Since  $\Delta h$  does not change under the quantum evolution, we can evaluate it using the initial cat state, which gives

$$(\Delta h)^2 = \frac{n^2}{4}. \quad (3.15)$$

The generalized-uncertainty bound becomes

$$\delta g \geq \delta g_c = \frac{1}{Tn\sqrt{\nu}} = \frac{1}{T\sqrt{Nn}} = \frac{\sqrt{\nu}}{TR(\tau - T)}. \quad (3.16)$$

By letting the probe qubits be in a collective entangled state, the accuracy in our estimate is enhanced by a factor of  $1/\sqrt{n}$ .

For the cat-state input with no decoherence, it is optimal to make  $\nu$  as small as possible, i.e.,  $\nu = \nu_{\min}$ . This puts as many qubits as possible into each probe consistent with the constraint (2.14), i.e.,  $n = N/\nu_{\min}$ , which is clearly optimal in the absence of any decoherence to degrade the entanglement. To find the optimal bound on the measurement accuracy, we adjust the interaction time  $T$  to minimize  $\delta g_c$ , giving

$$T = \frac{1}{2}\tau \quad (3.17)$$

and

$$N = n\nu_{\min} = \frac{1}{2}R\tau. \quad (3.18)$$

In order that  $\nu \geq \nu_{\min}$ , we require  $\frac{1}{2}R\tau \geq \nu_{\min}$ . When  $\frac{1}{2}R\tau < \nu_{\min}$ , we choose  $n = 1$  and  $\nu = \nu_{\min}$ , which gives  $T = T_s$  and an optimal bound that is the same as for product-state inputs.

The optimal bound on measurement accuracy thus becomes

$$\delta g_c = \begin{cases} \frac{1}{T_s\sqrt{\nu_{\min}}}, & 1 \leq R\tau < 2\nu_{\min}, \\ \frac{4\sqrt{\nu_{\min}}}{R\tau^2}, & R\tau \geq 2\nu_{\min}. \end{cases} \quad (3.19)$$

The  $1/R\tau^2$  scaling of the cat-state bound is the signature of the so-called *Heisenberg limit*; it is to be contrasted with the corresponding  $1/\sqrt{R\tau^3}$  scaling available from product states. The enhancement available from entanglement is roughly a factor of  $\sqrt{\nu_{\min}/R\tau}$ . Just as for product states, the behavior of the bound for  $1 \leq R\tau < 2\nu_{\min}$  is not so important, as it expresses what happens when the measurement protocol is starved of qubits.



### C. Achieving the optimal measurement accuracy

Estimating  $g$  involves making measurements on the probe qubits. A strategy that gives an optimal estimate of  $g$  is to measure  $\sigma_x$  on all the probe qubits. This provides a means of estimating  $gT$ , from which  $g$  can be calculated provided we know the interaction time  $T$  accurately.

In the case of an initial pure product state, we can specialize to having just one qubit in each probe ( $n = 1$ ), prepared in the state (3.3). We measure  $\sigma_x$  on each qubit. The results are averaged over  $\nu$  trials to get an accurate estimate for  $g$  [9]. The expectation value and variance of  $\sigma_x$  with respect to the evolved state in Eq. (3.5) are

$$\langle \sigma_x \rangle = \cos gT, \quad (\Delta \sigma_x)^2 = 1 - \cos^2 gT = \sin^2 gT. \quad (3.20)$$

The average of the results over  $\nu$  trials, which we denote  $\bar{\sigma}_x$ , has the same expectation value, but its variance decreases by a statistical factor of  $1/\nu$ , i.e.,  $\Delta \bar{\sigma}_x = |\sin gT|/\sqrt{\nu}$ .

We estimate  $g$  as  $g_{\text{est}} = T^{-1} \arccos \bar{\sigma}_x$ . When the uncertainty in  $\bar{\sigma}_x$  is small enough, we can approximate  $\langle g_{\text{est}} \rangle = T^{-1} \arccos \langle \bar{\sigma}_x \rangle = g$  and

$$\delta g = \Delta g_{\text{est}} = \frac{\Delta \bar{\sigma}_x}{|d\langle \bar{\sigma}_x \rangle / dg|} = \frac{1}{T\sqrt{\nu}}. \quad (3.21)$$

The approximation here is that the datum  $\bar{\sigma}_x$  must be likely to lie close enough to the expected value  $\langle \bar{\sigma}_x \rangle$  that a linear approximation to the arccos function at the operating point is valid. This requires that  $\nu$  be large enough that  $1 \gg \Delta \bar{\sigma}_x = \Delta \sigma_x / \sqrt{\nu} \sim 1/\sqrt{\nu}$ . That  $\nu$  must be large is the expression, in the context of this particular measurement, of the general fact that the quantum Cramer-Rao can only be achieved asymptotically; it leads to our requirement that  $\nu \geq \nu_{\text{min}} \gg 1$ .

When the probe is initialized in the cat state, an optimal measurement strategy is to measure  $\sigma_x$  on all  $n$  qubits simultaneously and to multiply all the results together [9]. Formally, this corresponds to measuring

$$\Sigma_x = \bigotimes_{j=1}^n \sigma_{x;j} \quad (3.22)$$

The expectation value and variance of  $\Sigma_x$  with respect to the evolved state (3.14) are

$$\langle \Sigma_x \rangle = \cos ngT, \quad (\Delta \Sigma_x)^2 = 1 - \cos^2 ngT = \sin^2 ngT. \quad (3.23)$$

The average of the results over  $\nu$  probes has the same expectation value, but its variance decreases by a statistical factor of  $1/\nu$ .

We estimate  $g$  in the same way as above for product inputs. The only difference is the additional factor of  $n$  in the rotation angle due to the coherent rotation of the entangled qubits in each probe. The resulting uncertainty in our estimate of  $g$  is

$$\delta g = \frac{1}{Tn\sqrt{\nu}}, \quad (3.24)$$

thus saturating the bound (3.16). Notice that the condition for making a linear approximation to the arccos function is the same as for product inputs, i.e.,  $1 \gg \Delta\bar{\Sigma}_x = \Delta\Sigma_x/\sqrt{\nu} \sim 1/\sqrt{\nu}$ , showing that we can take  $\nu_{\min}$  to have the same value for product and cat-state protocols.

There are technical questions associated with how one resolves the fringes in Eqs. (3.20) and (3.23) in order to zero in on the actual value of  $g$ . These questions are well understood, however, and are irrelevant to our goal of understanding the effects of decoherence, so we do not consider them further.

#### IV. MEASUREMENT ACCURACY IN THE PRESENCE OF DECOHERENCE

The previous section reviewed, within the context of our resource-based analysis, the measurement accuracies that can be obtained in the absence of decoherence. In this section we introduce decoherence to see how it affects the accuracy of parameter estimation. We consider a general model for decoherence of the probe qubits, subject to the restrictions that the decoherence (i) is independent and identical from one probe qubit to the next, (ii) is continuously differentiable and time stationary, and (iii) commutes with rotations about the  $\sigma_z$  axis. Since the interaction Hamiltonian that connects the probe qubits to the parameter generates rotations about the  $\sigma_z$  axis of each of the qubits, the effect of the third restriction is to separate cleanly the effect of the parameter from the effects of decoherence.

Decoherence can be described in terms of trace-preserving quantum operations (completely positive maps) on density operators [28, 29, 30, 31, 32, 33]. A quantum operation on single-qubit states is completely specified by the transformations of the operator basis set consisting of  $\mathbb{1}$ ,  $\sigma_x$ ,  $\sigma_y$ , and  $\sigma_z$ . A general time-dependent trace-preserving map  $\mathcal{A}_t$  on one-qubit states, which commutes with rotations about the  $\sigma_z$  axis, has the form

$$\begin{aligned}\mathcal{A}_t(\mathbb{1}) &= \mathbb{1} + f(t)\sigma_z, \\ \mathcal{A}_t(\sigma_z) &= g(t)\sigma_z, \\ \mathcal{A}_t(\sigma_x \pm i\sigma_y) &= h_{\pm}(t)(\sigma_x \pm i\sigma_y),\end{aligned}\tag{4.1}$$

where  $f(t)$ ,  $g(t)$ , and  $h_{+}(t) = h_{-}^{*}(t)$  are arbitrary functions of time  $t$ . The requirement that the evolution described by  $\mathcal{A}_t$  be continuously differentiable and time stationary implies that the derivatives of the quantities on the left of Eq. (4.1) be linear combinations with constant coefficients of these same quantities. Thus we have

$$\begin{aligned}\frac{d\mathcal{A}_t(\mathbb{1})}{dt} &= \mu\gamma_1\mathcal{A}_t(\sigma_z), \\ \frac{d\mathcal{A}_t(\sigma_z)}{dt} &= -\gamma_1\mathcal{A}_t(\sigma_z), \\ \frac{d\mathcal{A}_t(\sigma_x \pm i\sigma_y)}{dt} &= -(\gamma_2 \pm i\omega)\mathcal{A}_t(\sigma_x \pm i\sigma_y),\end{aligned}\tag{4.2}$$

where  $\mu$ ,  $\gamma_1$ ,  $\gamma_2$ , and  $\omega$  are real constants.

The solution of Eqs. (4.2), with  $\mathcal{A}_0 = \mathcal{I}$ , gives the most general single-qubit decoherence model that satisfies restrictions (ii) and (iii) above:

$$\begin{aligned}\mathcal{A}_t(\mathbb{1}) &= \mathbb{1} + \mu(1 - e^{-\gamma_1 t})\sigma_z, \\ \mathcal{A}_t(\sigma_z) &= e^{-\gamma_1 t}\sigma_z, \\ \mathcal{A}_t(\sigma_x \pm i\sigma_y) &= e^{-\gamma_2 t}e^{\mp i\omega t}(\sigma_x \pm i\sigma_y).\end{aligned}\tag{4.3}$$

The dissipation in this model is that of the standard qubit decoherence model, involving a longitudinal decay time  $T_1 = 1/\gamma_1$  and a transverse dephasing time  $T_2 = 1/\gamma_2$ . In the limit  $t \rightarrow \infty$ , every single-qubit state decays to the state  $\frac{1}{2}(\mathbb{1} + \mu\sigma_z)$ , which means that we must have  $-1 \leq \mu \leq 1$ . Complete positivity requires that  $T_2 \leq 2T_1$ .

In addition to the dissipation, there is a coherent rotation about the  $\sigma_z$  axis by an angle  $\omega t$ . If a decoherence process does introduce such a coherent rotation, it cannot be distinguished from the rotation produced by the parameter  $g$ ; any procedure for estimating  $g$  would actually estimate  $g + \omega$ . Throughout the following, we assume that the decoherence model does not include any coherent rotation, but for convenience, we incorporate the rotation due to  $g$  into  $\mathcal{A}_t$  by assuming that  $\omega = g$  and omitting the further coherent rotation in Eq. (2.1). The mapping of the Bloch sphere induced by  $\mathcal{A}_t$  (with  $\omega = g$ ) is illustrated in Fig. 1.

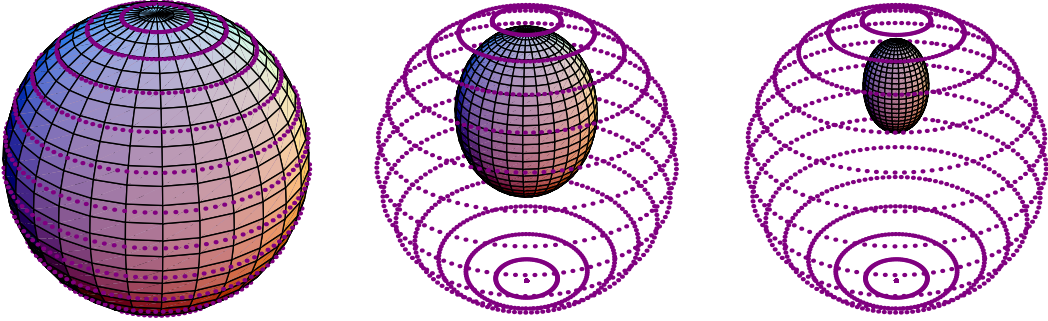


FIG. 1: (color online) The transformation of the Bloch sphere under the map  $\mathcal{A}_t$  of Eq. (4.3) at  $\gamma_2 t = 0$ ,  $\pi/4$  and  $\pi/2$ , with  $\mu = 3/4$  and  $\gamma_1 = 3\gamma_2/4$ . The dotted lines show the unit sphere. The coherent rotation due to  $\omega = g$  cannot be seen in these diagrams.

### A. Initial pure product state

We are now prepared to investigate how decoherence affects the theoretical minimum for  $\delta g$  when the probe is initialized in a product state. At time  $t$  after entering the quantum channel, the

state of a probe is given by applying the map (4.3) to the initial state of each qubit in the pure product state (3.4):

$$\rho_p(g, t) = \frac{1}{2^n} \bigotimes_{j=1}^n \left( \mathbb{1}_j + \mu(1 - e^{-\gamma_1 t}) \sigma_{z;j} + e^{-\gamma_2 t} (\sigma_{x;j} \cos gt + \sigma_{y;j} \sin gt) \right). \quad (4.4)$$

We first look at the weaker inequality in Eq. (2.13). At the time  $t = T$  when the probe leaves the quantum channel, we have  $\langle h_j \rangle_T = \frac{1}{2} \text{tr}[\rho_p(g, T) \sigma_{z;j}] = \mu(1 - e^{-\gamma_1 T})/2$  and  $\langle h_j^2 \rangle_T = 1/4$ , giving a variance

$$(\Delta h)^2 = n \langle h_j^2 \rangle_T = \frac{n}{4} \left( 1 - \mu^2 (1 - e^{-\gamma_1 T})^2 \right). \quad (4.5)$$

The resulting weaker uncertainty-principle bound from Eq. (2.13) is thus

$$\delta g \geq \delta g_p^{(w)}(\gamma_1) = \frac{1}{T\sqrt{N}} \frac{1}{\sqrt{1 - \mu^2 (1 - e^{-\gamma_1 T})^2}}. \quad (4.6)$$

Decoherence in the transverse  $(\sigma_{x;j} - \sigma_{y;j})$  plane does not appear explicitly in the bound  $\delta g_p^{(w)}(\gamma_1)$ . This is because the weaker inequality in Eq. (2.13) is determined by the variance of  $h$ , which depends only on the decoherence along the longitudinal  $\sigma_{z;j}$  direction.

Our conclusion is that we should not rely on the weaker inequality in Eq. (2.13) to provide a good bound on the maximum achievable measurement accuracy when there is decoherence. For instance, in the case where there is only transverse decoherence, i.e.,  $\gamma_1 = 0$ , the bound  $\delta g_p^{(w)}(\gamma_1)$  remains constant at  $1/T\sqrt{N}$ , even though the transverse decoherence ultimately leaves the probe qubits in a state along the  $\sigma_z$  axis where the rotation produced by the parameter has no effect. To see the dependence of the measurement accuracy on the transverse decoherence, we have to use the stronger inequality in Eq. (2.13).

Turning to that stronger inequality, we need to evaluate  $\Delta$  as in Eq. (2.11), and for that purpose, we first write the state of each probe qubit after passage through the channel in diagonal form,

$$\rho_j(g, T) = \frac{1}{2} \left( 1 + \sqrt{d_1^2 + d_2^2} \right) |+\rangle\langle+| + \frac{1}{2} \left( 1 - \sqrt{d_1^2 + d_2^2} \right) |-\rangle\langle-| \quad (4.7)$$

where

$$d_1 \equiv \mu(1 - e^{-\gamma_1 T}), \quad d_2 \equiv e^{-\gamma_2 T} \quad (4.8)$$

and

$$\begin{aligned} |+\rangle &\equiv \cos(\theta/2)|0\rangle + e^{igT} \sin(\theta/2)|1\rangle, \\ |-\rangle &\equiv \sin(\theta/2)|0\rangle - e^{igT} \cos(\theta/2)|1\rangle, \end{aligned} \quad (4.9)$$

are the eigenstates of  $\rho_j(g, T)$ , with

$$\sin \theta = \frac{d_2}{\sqrt{d_1^2 + d_2^2}}. \quad (4.10)$$

To evaluate  $\Delta_j$  for the  $j$ th qubit, we need the off-diagonal matrix element of  $h_j = \frac{1}{2}\sigma_{z;j}$  in this eigenbasis:

$$(h_j)_{+-} = (h_j)_{-+}^* = \frac{1}{2}\langle +|\sigma_{z;j}|-\rangle = \frac{1}{2}\sin\theta. \quad (4.11)$$

Plugging Eqs. (4.7) and (4.11) into Eq. (2.11), we find that

$$\Delta^2 = n\Delta_j^2 = \frac{n}{4}d_2^2 = \frac{n}{4}e^{-2\gamma_2 T}, \quad (4.12)$$

from which follows a stronger uncertainty-principle bound,

$$\delta g \geq \delta g_p^{(s)}(\gamma_2) = \frac{e^{\gamma_2 T}}{T\sqrt{N}} = \frac{e^{\gamma_2 T}}{T\sqrt{R(\tau - T)}}, \quad (4.13)$$

for  $\nu$  uses of the quantum probe. This is a much more reasonable bound on measurement accuracy, since it depends explicitly on the transverse decoherence that we expect to make a difference in the measurement; moreover, the dependence simply degrades the measurement accuracy exponentially with the number of  $T_2$  times for which each probe is in the quantum channel.

We can show that directly that the bound (4.6) is weaker than that of Eq. (4.13) through the following chain of inequalities:

$$\sqrt{1 - \mu^2(1 - e^{-\gamma_1 T})^2} \geq \sqrt{1 - (1 - e^{-\gamma_1 T})^2} = \sqrt{e^{-\gamma_1 T}(2 - e^{-\gamma_1 T})} \geq e^{-\gamma_1 T/2} \geq e^{-\gamma_2 T}, \quad (4.14)$$

the last of which requires the complete-positivity condition,  $\gamma_2 \geq \gamma_1/2$ .

Since the probe state is separable at all times, we can choose  $n = 1$  without affecting the optimal measurement. What remains is to choose the interaction time  $T$ , within the range  $0 \leq T \leq \tau$ , so as to minimize the bound  $\delta g_p^{(s)}(\gamma_2)$ . There is a single minimum at  $T = T_p$ , determined by the equation  $(\gamma_2 T_p)^2 - (3/2 + \gamma_2 \tau)\gamma_2 T_p + \gamma_2 \tau = 0$  to occur at

$$\gamma_2 T_p = \frac{3/2 + \gamma_2 \tau - \sqrt{(3/2 + \gamma_2 \tau)^2 - 4\gamma_2 \tau}}{2}. \quad (4.15)$$

We cannot use this interaction time when it becomes so short that the measurement protocol is starved of qubits, i.e., when  $R(\tau - T_p) < \nu_{\min}$ . In this situation, we choose  $n = 1$  and  $\nu = \nu_{\min}$ , which gives the interaction time  $T_s$  of Eq. (3.10).

Plugged into Eq. (4.13), these interaction times give the optimal value of the bound  $\delta g_p^{(s)}(\gamma_2)$ , which can be written in the dimensionless form

$$\sqrt{\frac{R}{\gamma_2}} \frac{\delta g_p^{(s)}(\gamma_2)}{\gamma_2} = \begin{cases} \sqrt{\frac{R}{\gamma_2}} \frac{e^{\gamma_2 T_s}}{\gamma_2 T_s \sqrt{\nu_{\min}}}, & \frac{\nu_{\min} \gamma_2}{R} \leq \gamma_2 \tau < \gamma_2 \left(T_p + \frac{\nu_{\min}}{R}\right), \\ \frac{e^{\gamma_2 T_p}}{\gamma_2 T_p \sqrt{\gamma_2(\tau - T_p)}}, & \gamma_2 \tau \geq \gamma_2 \left(T_p + \frac{\nu_{\min}}{R}\right). \end{cases} \quad (4.16)$$

We plot the dimensionless optimal interaction time,  $\gamma_2 T_p$ , and the resulting dimensionless optimal bound (4.16) as functions of  $\gamma_2 \tau$  in Fig. 2.

There are two important limits. When the transverse decoherence has little effect during the overall time  $\tau$ , i.e.,  $\gamma_2 \tau \ll 1$ , we find  $T_p = 2\tau/3$  and an optimal bound that reduces to the optimal

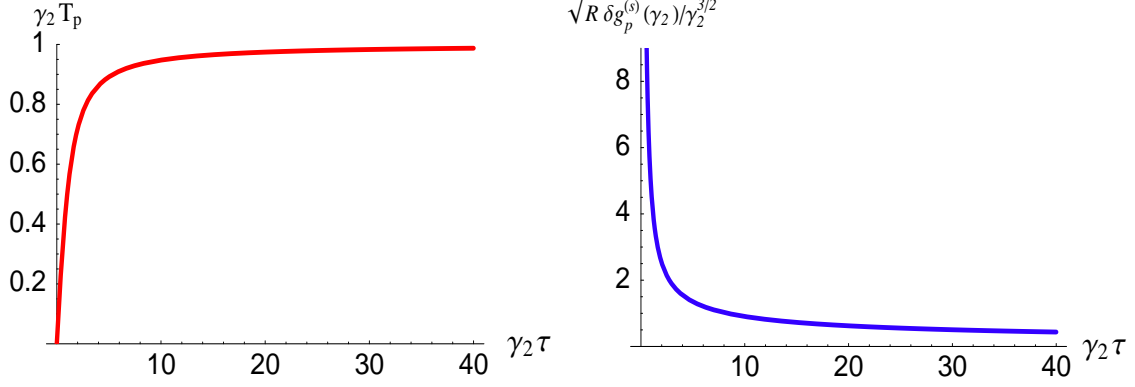


FIG. 2: Dimensionless optimal interaction time,  $\gamma_2 T_p$  of Eq. (4.15), and dimensionless optimal bound (4.16), plotted as functions of dimensionless interaction time  $\gamma_2 \tau$ . In these plots we assume that  $R$  is big enough that we do not encounter the situation where the protocol is starved of qubits, since this situation is of little interest.

measurement accuracy (3.11) in the absence of decoherence. In contrast, for large transverse decoherence, i.e.,  $\gamma_2 \tau \gg 1$ , the optimal interaction time is  $T_p = T_2$ , and the optimal bound becomes  $\delta g_p^{(s)}(\gamma_2) = e/T_2 \sqrt{R\tau}$  or, in terms of the dimensionless optimal bound,  $\sqrt{R/\gamma_2} \delta g_p^{(s)}/\gamma_2 = e/\sqrt{\gamma_2 \tau}$ . In this case, it is optimal to have each qubit scoot through the quantum channel in a dephasing time, before the dephasing can destroy the effect of the parameter-induced rotation; roughly speaking, each qubit determines  $g$  with accuracy  $e/T_2$ , which is improved by the statistical factor  $1/\sqrt{R\tau}$  corresponding to the number of qubits used in time  $\tau$ .

### B. Initial pure entangled state

We now look at the case in which the probe is initialized in an entangled cat state. The density operator of the probe, after a time  $t$  in the channel, is obtained by applying the map (4.3) to the initial cat state (3.13):

$$\begin{aligned} \rho_c(g, t) = & \frac{1}{2^{n+1}} \left( \bigotimes_{j=1}^n \left( \mathbb{1}_j + [e^{-\gamma_1 t} + \mu(1 - e^{-\gamma_1 t})] \sigma_{z;j} \right) + \bigotimes_{j=1}^n \left( \mathbb{1}_j - [e^{-\gamma_1 t} - \mu(1 - e^{-\gamma_1 t})] \sigma_{z;j} \right) \right. \\ & \left. + e^{-n\gamma_2 t - i n g t} \bigotimes_{j=1}^n (\sigma_{x;j} + i \sigma_{y;j}) + e^{-n\gamma_2 t + i n g t} \bigotimes_{j=1}^n (\sigma_{x;j} - i \sigma_{y;j}) \right). \end{aligned} \quad (4.17)$$

To evaluate the weaker inequality in Eq. (2.13), we need to evaluate the variance of  $h$ . Using Eqs. (B1), (B2) and (B3) from Appendix B, we find that at the time  $t = T$  when the probe exits the quantum channel,  $\langle h \rangle_T = n d_1/2$  and

$$\langle h^2 \rangle_T = \frac{n}{4} \left( 1 + (n-1)(e^{-2\gamma_1 T} + d_1^2) \right). \quad (4.18)$$

From these we obtain the variance of  $h$  at the time  $T$  when the probe exits the quantum channel:

$$(\Delta h)^2 = \langle \hat{h}^2 \rangle_T = \frac{n}{4} \left( 1 + (n-1)e^{-2\gamma_1 T} - d_1^2 \right). \quad (4.19)$$

The weaker bound in Eq. (2.13) on the accuracy of estimating  $g$  thus becomes

$$\delta g \geq \delta g_c^{(w)}(\gamma_1) = \frac{1}{T\sqrt{N}} \frac{1}{\sqrt{1 + (n-1)e^{-2\gamma_1 T} - \mu^2 (1 - e^{-\gamma_1 T})^2}}. \quad (4.20)$$

We do not expect this bound on  $\delta g_c(\gamma)$  to be particularly useful because, as for the case of an initial product state, the decoherence in the transverse directions for the qubits does not come into the bound at all.

We now look at the bound on measurement accuracy placed by the stronger inequality in Eq. (2.13). The density operator  $\rho_c(g, t)$  is diagonal in the tensor-product basis formed by the eigenvectors of  $\sigma_{z;j}$ , except in the two-dimensional subspace spanned by the vectors  $|00 \dots 0\rangle \equiv |\mathbf{0}\rangle$  and  $|11 \dots 1\rangle \equiv |\mathbf{1}\rangle$ . We denote this subspace of the  $n$ -qubit Hilbert space  $\mathcal{H}$  by  $\mathcal{K}$ . The operator  $h$  is diagonal in the tensor-product basis formed by eigenvectors of  $\sigma_{z;j}$ . From Eq. (2.11), we see that there is no contribution to  $\Delta^2$  from the subspace in which  $\rho_c(g, t)$  and  $h$  are simultaneously diagonal. Thus, for computing  $\Delta^2$ , we can work with the operators  $\bar{\rho}_c(g, t)$  and  $\bar{h}$  that are obtained by projecting  $\rho_c(g, t)$  and  $h$  down to the subspace  $\mathcal{K}$ , i.e.,

$$\bar{\rho}_c(g, T) = \frac{1}{2} \left( d_+ |\mathbf{0}\rangle \langle \mathbf{0}| + d_- |\mathbf{1}\rangle \langle \mathbf{1}| + d_2^n e^{-ingT} |\mathbf{0}\rangle \langle \mathbf{1}| + d_2^n e^{ingT} |\mathbf{1}\rangle \langle \mathbf{0}| \right) \quad (4.21)$$

and

$$\bar{h} = \frac{n}{2} (|\mathbf{0}\rangle \langle \mathbf{0}| - |\mathbf{1}\rangle \langle \mathbf{1}|), \quad (4.22)$$

with

$$d_{\pm} \equiv \left( \frac{1 + e^{-\gamma_1 T} \pm d_1}{2} \right)^n + \left( \frac{1 - e^{-\gamma_1 T} \pm d_1}{2} \right)^n. \quad (4.23)$$

The next step is to write  $\bar{\rho}_c(g, T)$  in diagonal form,

$$\bar{\rho}_c(g, T) = p_+ |+\rangle \langle +| + p_- |-\rangle \langle -|, \quad (4.24)$$

where

$$p_{\pm} = \frac{1}{4} \left( d_+ + d_- \pm \sqrt{(d_+ - d_-)^2 + 4d_2^{2n}} \right) \quad (4.25)$$

are the eigenvalues of  $\bar{\rho}_c$  and

$$\begin{aligned} |+\rangle &\equiv \cos(\theta/2) |\mathbf{0}\rangle + e^{ingT} \sin(\theta/2) |\mathbf{1}\rangle, \\ |-\rangle &\equiv \sin(\theta/2) |\mathbf{0}\rangle - e^{ingT} \cos(\theta/2) |\mathbf{1}\rangle, \end{aligned} \quad (4.26)$$

are the eigenstates, with

$$\sin \theta = \frac{2d_2^n}{\sqrt{(d_+ - d_-)^2 + 4d_2^{2n}}}. \quad (4.27)$$

To evaluate  $\Delta$ , we need the off-diagonal matrix element of  $\bar{h}$  in this eigenbasis:

$$\bar{h}_{+-} = \bar{h}_{-+}^* = \langle + | \bar{h} | - \rangle = \frac{n}{2} \sin \theta . \quad (4.28)$$

The resulting value of  $\Delta^2$  is

$$\Delta^2 = (p_+ - p_-)^2 |\bar{h}_{+-}|^2 = \frac{n^2}{4} e^{-2n\gamma_2 T} , \quad (4.29)$$

from which follows the stronger uncertainty-principle bound for a cat-state input,

$$\delta g \geq \delta g_c^{(s)}(\gamma_2) = \frac{e^{n\gamma_2 T}}{Tn\sqrt{\nu}} = \frac{e^{n\gamma_2 T}}{T\sqrt{nR(\tau-T)}} = \frac{\sqrt{\nu}e^{\gamma_2 RT(\tau-T)/\nu}}{RT(\tau-T)} \quad (4.30)$$

Aside from being stronger than the bound (4.20), this is a more sensible bound, since it depends explicitly on the transverse decoherence. When  $\gamma_2 = 0$ , this bound simplifies to the cat-state bound in the absence of decoherence, Eq. (3.16). Moreover, by comparing with the bound for a product input, Eq. (4.13), one sees that this bound retains the  $1/\sqrt{n}$  advantage purchased by using an entangled input, but at the price of a decoherence rate that is  $n$  times faster.

We have assumed that both  $n$  and  $T$  are controllable parameters in the estimation scheme we are considering, with  $\nu$  determined by Eq. (1.4). To minimize the bound (4.20), we use the second form, from which  $\nu$  has been eliminated. The values for  $n$  and  $T$  that minimize  $\delta g_c^{(s)}$  can then be found by solving simultaneously the two equations,

$$\begin{aligned} 0 &= \frac{\partial \delta g_c^{(s)}}{\partial n} = \frac{e^{n\gamma_2 T}}{2nT\sqrt{nR(\tau-T)}}(2n\gamma_2 T - 1) , \\ 0 &= \frac{\partial \delta g_c^{(s)}}{\partial T} = \frac{e^{n\gamma_2 T}}{2T^2(\tau-T)\sqrt{nR(\tau-T)}}[3T + 2n\gamma_2 T(\tau-T) - 2\tau] , \end{aligned} \quad (4.31)$$

which give  $n = 1/\gamma_2\tau$  and  $T = \tau/2$ . The determinant and trace of the Hessian of  $\delta g_c^{(s)}$ , with respect to  $n$  and  $T$ , evaluated at this point, are both positive, showing that it is indeed a minimum. The minimum value of the bound is

$$\delta g_c^{(s)}(\gamma_2) = \frac{2\sqrt{2e}}{\tau\sqrt{R/\gamma_2}} . \quad (4.32)$$

This minimum cannot always be attained, however, because we have the additional constraints of Eq. (2.14), i.e.,  $1 \leq n \leq N/\nu_{\min} = R(\tau-T)/\nu_{\min} = R\tau/2\nu_{\min}$ , which do not always allow us to choose  $n$  equal to the optimal value  $1/\gamma_2\tau$ . If  $\gamma_2\tau$  does not lie between  $2\nu_{\min}/R\tau$  and 1, we have to choose a value for  $n$  that lies on the boundary of allowed values. There are two cases to consider. If the decoherence rate is high, i.e.,  $\gamma_2\tau \geq 1$ , we choose  $n = 1$ , thus using probes consisting of individual qubits to estimate  $g$ , in which case the analysis reduces to that of the preceding subsection. Notice that  $\gamma_2\tau = 1$  gives  $\gamma_2(T_p + \nu_{\min}/R) = 1/2 + \nu_{\min}\gamma_2/R$ . Thus if  $2\nu_{\min}\gamma_2/R \leq 1$ , the second case in Eq. (4.16) applies whenever  $\gamma_2\tau \geq 1$ . If, however,  $2\nu_{\min}\gamma_2/R > 1$ , the protocol begins to be starved of qubits for some  $\gamma_2\tau > 1$ , and there is no situation where cat states offer any advantage. Throughout the following, therefore, we assume that  $2\nu_{\min}\gamma_2/R \leq 1$ .



TABLE I: Minimum value of bound on estimating  $g$  using cat-state probes with available resources deployed optimally. The table assumes that  $2\nu_{\min}\gamma_2/R \leq 1$ .

Range of $\gamma_2\tau$	$T$	$n$	$\nu$	$N$	$\delta g_c^{(s)}(\gamma_2)$
$\frac{\nu_{\min}\gamma_2}{R} \leq \gamma_2\tau < \frac{2\nu_{\min}\gamma_2}{R}$	$T_s$ of Eq. (3.10)	1	$\nu_{\min}$	$\nu_{\min}$	$\frac{e^{\gamma_2 T_s}}{T_s \sqrt{\nu_{\min}}}$
$\frac{2\nu_{\min}\gamma_2}{R} \leq \gamma_2\tau < \sqrt{\frac{2\nu_{\min}\gamma_2}{R}}$	$\tau/2$	$R\tau/2\nu_{\min}$	$\nu_{\min}$	$R\tau/2$	$\frac{4\sqrt{\nu_{\min}}}{R\tau^2} e^{\gamma_2 R\tau^2/4\nu_{\min}}$
$\sqrt{\frac{2\nu_{\min}\gamma_2}{R}} \leq \gamma_2\tau < 1$	$\tau/2$	$1/\gamma_2\tau$	$\gamma_2 R\tau^2/2$	$R\tau/2$	$\frac{2\sqrt{2}e}{\tau \sqrt{R/\gamma_2}}$
$\gamma_2\tau \geq 1$	$T_p$ of Eq. (4.15)	1	$R(\tau - T_p)$	$R(\tau - T_p)$	$\frac{e^{\gamma_2 T_p}}{T_p \sqrt{R(\tau - T_p)}}$

If the decoherence is small, i.e.,

$$\gamma_2\tau < 2\nu_{\min}/R\tau \iff \tau^2 < 2\nu_{\min}/\gamma_2 R, \quad (4.33)$$

we use the largest cat state that can be constructed from the available resources, thus choosing  $\nu = \nu_{\min}$ . Using the last form in Eq. (4.30), with  $\nu = \nu_{\min}$ , we find that  $\delta g_c^{(s)}$  has extrema for  $T(\tau - T) = \nu_{\min}/\gamma_2 R$  and  $T = \tau/2$ . We discard the first possibility because it is inconsistent with the constraint (4.33), i.e.,  $\nu_{\min}/\gamma_2 R = T(\tau - T) \leq \tau^2/4 < \nu_{\min}/2\gamma_2 R$ . Moreover, the second derivative of  $\delta g_c^{(s)}$  with respect to  $T$ , evaluated at  $T = \tau/2$ , is strictly positive when Eq. (4.33) is satisfied, showing that  $T = \tau/2$  gives a minimum. The optimal interaction time is again  $T = \tau/2$  ( $n = R\tau/2\nu_{\min}$ ), and the minimum value of the bound becomes

$$\delta g_c^{(s)}(\gamma_2) = \frac{4\sqrt{\nu_{\min}}}{R\tau^2} e^{\gamma_2 R\tau^2/4\nu_{\min}}. \quad (4.34)$$

Notice that Eq. (4.34) reduces to the second case in Eq. (3.19) when there is no decoherence, i.e., when  $\gamma_2 = 0$ .

The first case in Eq. (3.19) reminds us that one further case occurs at very short times, when the protocol is starved of qubits. In particular, when  $R\tau/2\nu_{\min} < 1$ , we must choose  $n = 1$  and  $\nu = \nu_{\min}$ , leading to the familiar interaction time  $T_s$  of Eq. (3.10).

We can now piece together the various regions that govern the optimal bound on the estimate of  $g$  using cat-state probes with the available resources deployed in the optimal fashion. The results are summarized in Table I. The top row is the case where the protocol is starved of qubits; the second row is the case of low decoherence, for which the probes are prepared in cat states containing as many qubits as allowed by the need to have at least  $\nu_{\min}$  probes; the bottom row is the case of high decoherence, for which the probes are individual qubits; and the middle row describes the transition from high decoherence to low decoherence. The two regions where cat states play a role

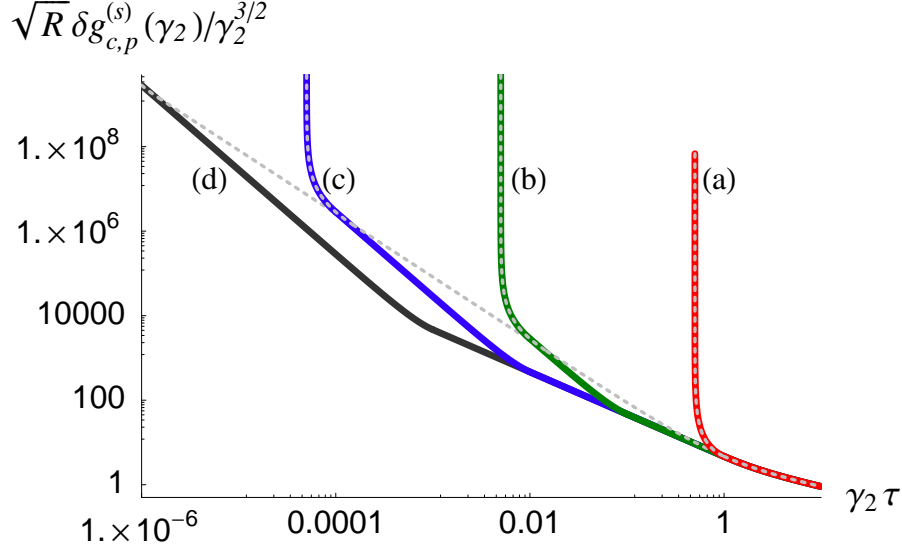


FIG. 3: (color online) The four thick lines labeled (a), (b), (c), and (d) show the dimensionless optimal bound (4.35) for cat-state inputs, plotted as a function of dimensionless interaction time  $\gamma_2 \tau$ , for  $\nu_{\min} = 50$  and  $\sqrt{R/2\nu_{\min}\gamma_2} = 1, 10, 100$ , and  $1000$ , i.e.,  $\sqrt{R/\gamma_2} = 10, 100, 1000$ , and  $10000$ , respectively. Note that both axes use a logarithmic scale. The use of cat states provides no advantage for  $\gamma_2 \tau \geq 1$ . The two regions where cat states provide an advantage (second and third rows of Table I) are absent for  $\sqrt{R/2\nu_{\min}\gamma_2} = 1$ , but become apparent for the other three values of  $\sqrt{R/2\nu_{\min}\gamma_2}$ . In terms of the dimensionless bound, the transition region between high and low decoherence (third row in Table I) has a form independent of  $R/\gamma_2$ , but extends to smaller values of  $\gamma_2 \tau$  as  $R/\gamma_2$  increases. For small enough  $\gamma_2 \tau$ , the protocol is starved of qubits, and cat states again provide no advantage over product states. The thin dotted lines show the dimensionless product-state bound (4.16) for the same four values of  $\sqrt{R/2\nu_{\min}\gamma_2}$ . The product-state bound agrees with the cat-state bound in the high-decoherence region ( $\gamma_2 \tau \geq 1$ ) and with the corresponding cat-state bound in the region where the protocol is starved of qubits ( $\nu_{\min}\gamma_2/R \leq \gamma_2 \tau < 2\nu_{\min}\gamma_2/R$ ); in between, where cat states provide an advantage, the product-state bound is independent of  $R/\gamma_2$ .

exist when  $2\nu_{\min}\gamma_2/R < 1$ . The dimensionless bound introduced in Eq. (4.16) is given by

$$\sqrt{\frac{R}{\gamma_2}} \frac{\delta g_c^{(s)}(\gamma_2)}{\gamma_2} = \begin{cases} \sqrt{\frac{R}{\gamma_2}} \frac{e^{\gamma_2 T_s}}{\gamma_2 T_s \sqrt{\nu_{\min}}} , & \frac{\nu_{\min}\gamma_2}{R} \leq \gamma_2 \tau < \frac{2\nu_{\min}\gamma_2}{R} , \\ \sqrt{\frac{\gamma_2}{R}} \frac{4\sqrt{\nu_{\min}}}{(\gamma_2 \tau)^2} e^{(R/\gamma_2)(\gamma_2 \tau)^2/4\nu_{\min}} , & \frac{2\nu_{\min}\gamma_2}{R} \leq \gamma_2 \tau < \sqrt{\frac{2\nu_{\min}\gamma_2}{R}} , \\ \frac{2\sqrt{2}e}{\gamma_2 \tau} , & \sqrt{\frac{2\nu_{\min}\gamma_2}{R}} \leq \gamma_2 \tau < 1 , \\ \frac{e^{\gamma_2 T_p}}{\gamma_2 T_p \sqrt{\gamma_2(\tau - T_p)}} , & \gamma_2 \tau \geq 1 . \end{cases} \quad (4.35)$$

This dimensionless optimal bound is plotted in Fig. 3 for the choice  $\nu_{\min} = 50$  and for several values of  $\sqrt{R/\gamma_2}$ .

The conclusion to be reached from the results summarized in Table I and Fig. 3 is that cat-state entanglement is only useful for improving the estimate of  $g$  when one wants to estimate  $g$  on a time scale that is shorter than the time scale over which decoherence acts.

### C. Achieving the optimal measurement accuracy

We now examine the effectiveness of the measurement strategies described in Sec. III C in the presence of decoherence in the probe qubits. When the input state is a product state, we can again specialize to the case where there is only one qubit in each probe ( $n = 1$ ) and  $\nu = N$ . We measure  $\sigma_x$  on each qubit and average over the results of  $\nu$  trials to obtain the estimate of  $g$ . After an interaction time  $t = T$ , the expectation value and variance of  $\sigma_x$  for a single qubit in the evolved state (4.4) are

$$\langle \sigma_x \rangle = e^{-\gamma_2 T} \cos gT, \quad (\Delta \sigma_x)^2 = 1 - e^{-2\gamma_2 T} \cos^2 gT. \quad (4.36)$$

Averaging over the results of  $\nu$  trials yields the quantity  $\bar{\sigma}_x$ , which has the same expectation value as  $\sigma_x$ , but has variance reduced to  $(\Delta \bar{\sigma}_x)^2 = (\Delta \sigma_x)^2 / \nu$ , and we estimate  $g$  as  $g = g_{\text{est}} = T^{-1} \arccos(e^{\gamma_2 T} \bar{\sigma}_x)$ . After many trials, the variance of  $\bar{\sigma}_x$  becomes small enough that we can approximate  $\langle g_{\text{est}} \rangle = T^{-1} \arccos(e^{\gamma_2 T} \langle \bar{\sigma}_x \rangle) = g$  and

$$\delta g = \Delta g_{\text{est}} = \frac{\Delta \bar{\sigma}_x}{|d\langle \bar{\sigma}_x \rangle / dg|} = \frac{e^{\gamma_2 T}}{T\sqrt{\nu}} \frac{\sqrt{1 - e^{-2\gamma_2 T} \cos^2 gT}}{|\sin gT|}. \quad (4.37)$$

If we use this straightforward method of estimating  $g$  by averaging measurements of  $\sigma_x$  on all qubits, achieving the bound (4.13) for determining  $g$ , with the interaction time adjusted to the optimal value  $T = T_p$ , requires  $|\sin gT_p| = 1$ . Even though  $g$  is not known, this can be accomplished by using feedback onto the rotation of the qubits to find this sweet spot on the fringe pattern. An alternative to feeding back onto the rotation of the qubits is feedback to rotate the quantity measured in the equatorial plane of the Bloch sphere until the desired operating point is achieved.

When the probe is initialized in a cat state, we have seen that the optimal strategy, in the absence of decoherence, is to measure  $\sigma_x$  on all  $n$  qubits simultaneously. The same measurement works when there is decoherence. Using Eqs. (3.22) and (4.17), we find that after an interaction time  $t = T$ ,

$$\langle \Sigma_x \rangle = e^{-n\gamma_2 T} \cos ngT, \quad (\Delta \Sigma_x)^2 = 1 - e^{-2n\gamma_2 T} \cos^2 ngT. \quad (4.38)$$

We can convert the results for product-state inputs to this case by the substitution  $T \rightarrow nT$ , so the average over  $\nu$  probes leads to

$$\delta g = \frac{e^{n\gamma_2 T}}{Tn\sqrt{\nu}} \frac{\sqrt{1 - e^{-2n\gamma_2 T} \cos^2 ngT}}{|\sin ngT|}. \quad (4.39)$$

We can saturate the bound (4.30) on estimating  $g$ , for the appropriate interaction time  $T$ , by using feedback to operate at a point where  $|\sin ngT| = 1$ .

One last point concerns the question of making a linear approximation to the arccos function, which allows us to relate the mean and variance of  $g_{\text{est}}$  directly to the mean and variance of  $\bar{\Sigma}_x$ . This approximation requires that  $\nu$  be large enough that  $1 \gg e^{n\gamma_2 T} \Delta \bar{\Sigma}_x = e^{n\gamma_2 T} \Delta \Sigma_x / \sqrt{\nu}$ . The results summarized in Table I show that for the optimal choices of  $n$  and  $T$ , it is always true that  $n\gamma_2 T \sim 1$ , showing that the requirement is that  $\nu$  be large in a way that is independent of the details of the protocol.

## V. DISCUSSION

In this paper we have studied quantum limits on determining a frequency  $g$  that controls the rate at which qubits rotate about the  $z$  axis of the Bloch sphere. The question of determining  $g$  is the same as the problem of distinguishing qubit states that differ by having been subjected to different rotations. The quantum limits on determining  $g$  are well known [9]: if  $n$  qubits are prepared in product states, the uncertainty in determining  $g$  scales as  $1/\sqrt{n}$ , the standard quantum limit or shot-noise limit, whereas if the same  $n$  qubits are prepared in an entangled cat state, the uncertainty scales as  $1/n$ , which is called the Heisenberg limit. Our purpose in this paper has been to investigate, following [10], how these scalings change when the qubits are subjected to independent, but identical decoherence processes during the measurement.

The decoherence model we consider is the most general continuous-time process that is invariant under rotations about the  $z$  axis. This results in a standard qubit decoherence model in which qubits decay with a time constant  $T_1$  and lose phase coherence with a time constant  $T_2$ . It is the phase-coherence time  $T_2$  that is important for efforts to estimate  $g$ ; cat-state entanglement is only useful for times of order or smaller than  $T_2$ .

To make the analysis meaningful, we introduce as resources the rate  $R$  at which qubits are supplied and the overall time  $\tau$  that one has available for estimating  $g$ . If one does not introduce these resources, one can achieve any desired accuracy in estimating  $g$  by assuming that one can assemble an arbitrarily large number of qubits in a cat state in a time much shorter than  $T_2$  or, more easily, by assuming that one can take as long as desired to determine  $g$  using an arbitrarily large number of qubits prepared in a product state. Once decoherence becomes a consideration, the uncertainty in estimating  $g$  should be written in terms of the decoherence time  $T_2$  and the relevant resources,  $R$  and  $\tau$ , not directly in terms of the number of qubits used.

The results of our analysis, summarized in Table I and Fig. 3, show that cat-state entanglement is useless if  $\tau \geq T_2$ . When  $T_2$  is much larger than  $\tau$ , the results show that one should put as many qubits as possible in each cat-state probe. For intermediate decoherence, it is not that cat-state entanglement is useless, but rather that one should make a judicious, optimal choice of how many qubits to include in each cat-state probe. The overall conclusion is that entanglement is only useful when one can make the effects of decoherence small on the time scale over which one must estimate  $g$ . While this conclusion is reached here for a special model of measurements on qubits, it is generally true for quantum-limited measurements in the face of decoherence.

Our analysis highlights one further point, having to do with using the quantum Cramer-Rao bound to determine quantum limits. As long as one is interested only in measurements involving pure states, the form of the Cramer-Rao bound as a generalized uncertainty principle is sufficient for investigating bounds on measurement accuracy. Once decoherence is introduced, however, inevitably leading to measurements on mixed states, one must use the stronger form of the Cramer-Rao bound involving the Fisher information to obtain meaningful bounds on measurement accuracy.

### Acknowledgments

This work was supported in part by U.S. Office of Naval Research Contract No. N00014-07-1-0304. We thank S. Boixo and A. Datta for useful suggestions and discussions.

### APPENDIX A: GENERALIZED UNCERTAINTY RELATIONS FOR PRODUCT STATES

Consider a continuous trajectory in the space of product states of  $n$  qubits parametrized by  $X$ ,

$$\rho_p(X) = \bigotimes_{j=1}^n \rho_j(X) , \quad (\text{A1})$$

If the value of  $X$  changes by a small amount  $dX$ , the change in  $\rho_j$  can be written as

$$\rho_j \rightarrow \rho_j + dX \rho'_j = \sum_{\alpha_j} dp_{\alpha_j} |\alpha_j\rangle\langle\alpha_j| + e^{-ih_j dX} \rho_j e^{ih_j dX} . \quad (\text{A2})$$

The vectors  $\{|\alpha_j\rangle\}$  make up the eigenbasis of  $\rho_j$ , with eigenvalues  $p_{\alpha_j}$ , i.e.,

$$\rho_j = \sum_{\alpha_j} p_{\alpha_j} |\alpha_j\rangle\langle\alpha_j| . \quad (\text{A3})$$

The operators  $h_j$  are the generators of translations in  $X$  for each of the  $n$  systems, while  $dp_{\alpha_j}$  are small changes in the eigenvalues of  $\rho_j$  due to the small change in  $X$ . Notice that in the presentation of Sec. II, the fact that  $\mathcal{A}_T$  is independent of the parameter  $g$  means that the eigenvalues of  $\rho(g, T)$  do not change with  $g$ ; thus the terms having to do with eigenvalue changes do not appear in that discussion.

Keeping terms to linear order in  $dX$ , we have

$$\rho'_j = \sum_{\alpha_j} \frac{dp_{\alpha_j}}{dX} |\alpha_j\rangle\langle\alpha_j| - i[h_j, \rho_j] . \quad (\text{A4})$$

The corresponding change in the overall state,

$$\rho_p \rightarrow \rho_p + dX \rho'_p = \rho_p + dX \sum_{j=1}^n \rho'_j \bigotimes_{k \neq j} \rho_k , \quad (\text{A5})$$

gives us

$$\rho'_p = \sum_{j=1}^n \left[ \sum_{\alpha_j} \frac{dp_{\alpha_j}}{dX} |\alpha_j\rangle\langle\alpha_j| - i[h_j, \rho_j] \right] \bigotimes_{k \neq j} \rho_k . \quad (\text{A6})$$

Our objective is to obtain an expression for a line element  $ds_p^2$  in the space of density operators  $\rho_p$  that measures the distinguishability of neighboring quantum states. Following Eq. (2.5), we have

$$\left( \frac{ds_p}{dX} \right)^2 = \text{tr} \left[ \rho'_p \mathcal{L}_{\rho_p}(\rho'_p) \right] . \quad (\text{A7})$$

We start by computing  $\mathcal{L}_{\rho_p}(\rho'_p)$  using the definition in Eq. (2.6). Noting that  $\rho_p$  is diagonal in the tensor product basis furnished by  $\{|\alpha_j\rangle\}$  for each of the systems and using Eq. (A6) we obtain

$$\begin{aligned} \mathcal{L}_{\rho_p}(\rho'_p) &= \sum_{\beta_1, \beta_2, \dots, \beta_n} \sum_{\delta_1, \delta_2, \dots, \delta_n} \frac{2}{p_{\beta_1} \cdots p_{\beta_n} + p_{\delta_1} \cdots p_{\delta_n}} \\ &\quad \times \left\langle \beta_1 \cdots \beta_n \left| \sum_{j=1}^n \left[ \sum_{\alpha_j} \frac{dp_{\alpha_j}}{dX} |\alpha_j\rangle \langle \alpha_j| - i[h_j, \rho_j] \right] \bigotimes_{k \neq j} \rho_k \right| \delta_1 \cdots \delta_n \right\rangle |\beta_1 \cdots \beta_n\rangle \langle \delta_1 \cdots \delta_n|. \end{aligned} \quad (\text{A8})$$

Simplifying this expression gives

$$\begin{aligned} \mathcal{L}_{\rho_p}(\rho'_p) &= \sum_{j=1}^n \left[ \sum_{\alpha_j} \frac{(dp_{\alpha_j}/dX)}{p_{\alpha_j}} |\alpha_j\rangle \langle \alpha_j| + 2i \sum_{\alpha_j, \beta_j} \frac{p_{\alpha_j} - p_{\beta_j}}{p_{\alpha_j} + p_{\beta_j}} [h_j]_{\alpha_j \beta_j} |\alpha_j\rangle \langle \beta_j| \right] \bigotimes_{k \neq j} \mathbb{1}_k \\ &= \sum_{\alpha=1}^n \mathcal{L}_{\rho_j}(\rho'_j) \bigotimes_{k \neq j} \mathbb{1}_k, \end{aligned} \quad (\text{A9})$$

which leads to

$$\left( \frac{ds_p}{dX} \right)^2 = \sum_{j=1}^n \text{tr}[\rho'_j \mathcal{L}_{\rho_j}(\rho'_j)] \times \prod_{k \neq j} \text{tr} \rho_k = \sum_{j=1}^n \text{tr}[\rho'_j \mathcal{L}_{\rho_j}(\rho'_j)] = \sum_{j=1}^n \left( \frac{ds_j}{dX} \right)^2, \quad (\text{A10})$$

where we use  $\text{tr} \rho'_j = 0$ . In the special case where all  $\rho_j$  are identical and equal to  $\rho$  and when changes in  $X$  affect all the systems in the same way, we have

$$\frac{ds_p}{dX} = \sqrt{n} \frac{ds}{dX} \quad \text{where} \quad \left( \frac{ds}{dX} \right)^2 = \text{tr}[\rho' \mathcal{L}_\rho(\rho')]. \quad (\text{A11})$$

## APPENDIX B: USEFUL IDENTITIES INVOLVING PAULI OPERATORS

A few identities involving products of Pauli operators that are used in our calculations are listed below:

$$\begin{aligned} \left( \sum_{j=1}^n \sigma_{z;j} \bigotimes_{j \neq k} \mathbb{1}_k \right) \bigotimes_{j=1}^n (\mathbb{1}_j \pm \sigma_{z;j}) &= \pm n \bigotimes_{j=1}^n (\mathbb{1}_j \pm \sigma_{z;j}), \\ \left( \sum_{j=1}^n \sigma_{z;j} \bigotimes_{j \neq k} \mathbb{1}_k \right) \bigotimes_{j=1}^n (\sigma_{x;j} \pm i\sigma_{y;j}) &= \pm n \bigotimes_{j=1}^n (\sigma_{x;j} \pm i\sigma_{y;j}), \\ \left( \sum_{j \neq k=1}^n \sigma_{z;j} \otimes \sigma_{z;k} \bigotimes_{l \neq j,k} \mathbb{1}_l \right) \bigotimes_{j=1}^n (\mathbb{1}_j \pm \sigma_{z;j}) &= (n^2 - n) \bigotimes_{j=1}^n (\mathbb{1}_j \pm \sigma_{z;j}), \\ \left( \sum_{j \neq k=1}^n \sigma_{z;j} \otimes \sigma_{z;k} \bigotimes_{l \neq j,k} \mathbb{1}_l \right) \bigotimes_{j=1}^n (\sigma_{x;j} \pm i\sigma_{y;j}) &= (n^2 - n) \bigotimes_{j=1}^n (\sigma_{x;j} \pm i\sigma_{y;j}), \end{aligned} \quad (\text{B1})$$

$$\left( \sum_{j=1}^n \sigma_{z;j} \bigotimes_{j \neq k} \mathbb{1}_k \right) \bigotimes_{j=1}^n (\mathbb{1}_j \pm A \sigma_{z;j}) = \pm A \sum_{j=1}^n (\mathbb{1}_j \pm A^{-1} \sigma_{z;j}) \bigotimes_{j \neq k=1}^n (\mathbb{1}_k \pm A \sigma_{z;k}), \quad (\text{B2})$$

$$\left( \sum_{j \neq k=1}^n \sigma_{z;j} \otimes \sigma_{z;k} \bigotimes_{l \neq j,k} \mathbb{1}_l \right) \bigotimes_{j=1}^n (\mathbb{1}_j \pm A \sigma_{z;j}) = A^2 \sum_{j \neq k=1}^n \left( \mathbb{1}_j \pm A^{-1} \sigma_{z;j} \right) \otimes \left( \mathbb{1}_k \pm A^{-1} \sigma_{z;k} \right) \bigotimes_{l \neq j,k} (\mathbb{1}_l \pm A \sigma_{z;l}) . \quad (\text{B3})$$


---

- [1] C. W. Helstrom, *Quantum detection and estimation theory*, vol. 123 of *Mathematics in science and engineering* (Academic Press, New York, 1976), 1st ed.
- [2] A. S. Holevo, *Probabilistic and statistical aspects of quantum theory*, vol. 1 of *North-Holland series in statistics and Probability theory* (North-Holland, Amsterdam, 1982), 1st ed.
- [3] S. L. Braunstein and C. M. Caves, Phys. Rev. Lett **72**, 3439 (1994).
- [4] S. L. Braunstein and C. M. Caves, in *Fundamental problems in quantum theory*, edited by D. Greenberger and A. Zeilinger (The New York Academy of Sciences, New York, 1995), vol. 755 of *Annals of the New York Academy of Sciences*, pp. 786–797.
- [5] S. L. Braunstein and C. M. Caves, in *Quantum communications and measurement*, edited by V. P. Belavkin, O. Hirota, and R. L. Hudson (Plenum Press, New York, 1995), pp. 21–30.
- [6] S. L. Braunstein, C. M. Caves, and G. J. Milburn, Ann. Phys. **247**, 135 (1996).
- [7] S. Boixo, S. T. Flammia, C. M. Caves, and J. Geremia, Phys. Rev. Lett. **98**, 090401 (2007).
- [8] E. Knill, G. Ortiz, and R. D. Somma, Phys. Rev. A **75**, 012328 (2007).
- [9] V. Giovannetti, S. Lloyd, and L. Maccone, Phys. Rev. Lett **96**, 010401 (2006).
- [10] S. F. Huelga, C. Macchiavello, T. Pellizzari, and A. K. Ekert, Phys. Rev. Lett. **79**, 3865 (1997).
- [11] R. Jozsa, D. S. Abrams, J. P. Dowling, and C. P. Williams, Phys. Rev. Lett. **85**, 2010 (2000).
- [12] I. L. Chuang, Phys. Rev. Lett. **85**, 2006 (2000).
- [13] J. Preskill, e-print quant-ph/001098 (2000).
- [14] M. Revzen and A. Mann, Phys. Lett. A **312**, 11 (2003).
- [15] M. de Burgh and S. D. Bartlett, Phys. Rev. A **72**, 042301 (2005).
- [16] S. Boixo, C. M. Caves, A. Datta, and A. Shaji, Laser Phys. **16**, 1525 (2006).
- [17] E. Bagan, M. Baig, and R. Muñoz Tapia, Phys. Rev. Lett. **87**, 257903 (2001).
- [18] G. Chiribella, G. M. D’Ariano, P. Perinotti, and M. F. Sacchi, Phys. Rev. Lett. **93**, 180503 (2004).
- [19] C. C. Gerry and R. A. Campos, Phys. Rev. A **68**, 025602 (2003).
- [20] J. A. Dunningham and K. Burnett, Phys. Rev. A **70**, 033601 (2004).
- [21] H. Wang and T. Kobayashi, Phys. Rev. A **71**, 021802 (2005).
- [22] J. J. Bollinger, W. M. Itano, D. J. Wineland, and D. J. Heinzen, Phys. Rev. A **54**, R4649 (1996).
- [23] P. Cappelaro, J. Emerson, N. Boulant, C. Ramanathan, S. Lloyd, and D. G. Cory, Phys. Rev. Lett. **94**, 020502 (2005).
- [24] V. Giovannetti, S. Lloyd, and L. Maccone, Science **306**, 1330 (2004).
- [25] V. Giovannetti, S. Lloyd, and L. Maccone, Phys. Rev. A **65**, 022309 (2002).
- [26] H. Cramer, *Mathematical methods of statistics* (Princeton Univ. Press, Princeton, 1946).
- [27] S. L. Braunstein, Nature **440**, 617 (2006).
- [28] E. C. G. Sudarshan, P. M. Mathews, and J. Rau, Phys. Rev. **121**, 920 (1961).
- [29] E. Størmer, Acta Math. **110**, 233 (1963).
- [30] K. Kraus, Ann. Phys. **64**, 311 (1971).
- [31] E. B. Davies, *Quantum theory of open systems* (Academic Press, New York, 1976).

- [32] H. P. Breuer and F. Petruccione, *The theory of open quantum systems* (Oxford university press, New York, 2002).
- [33] M. A. Nielsen and I. L. Chuang, *Quantum Computation and Quantum Information* (Cambridge University Press, Cambridge, 2000).